

YMTHE, Volume 26

Supplemental Information

**Altered Peptide Ligands Impact the Diversity
of Polyfunctional Phenotypes in T Cell Receptor
Gene-Modified T Cells**

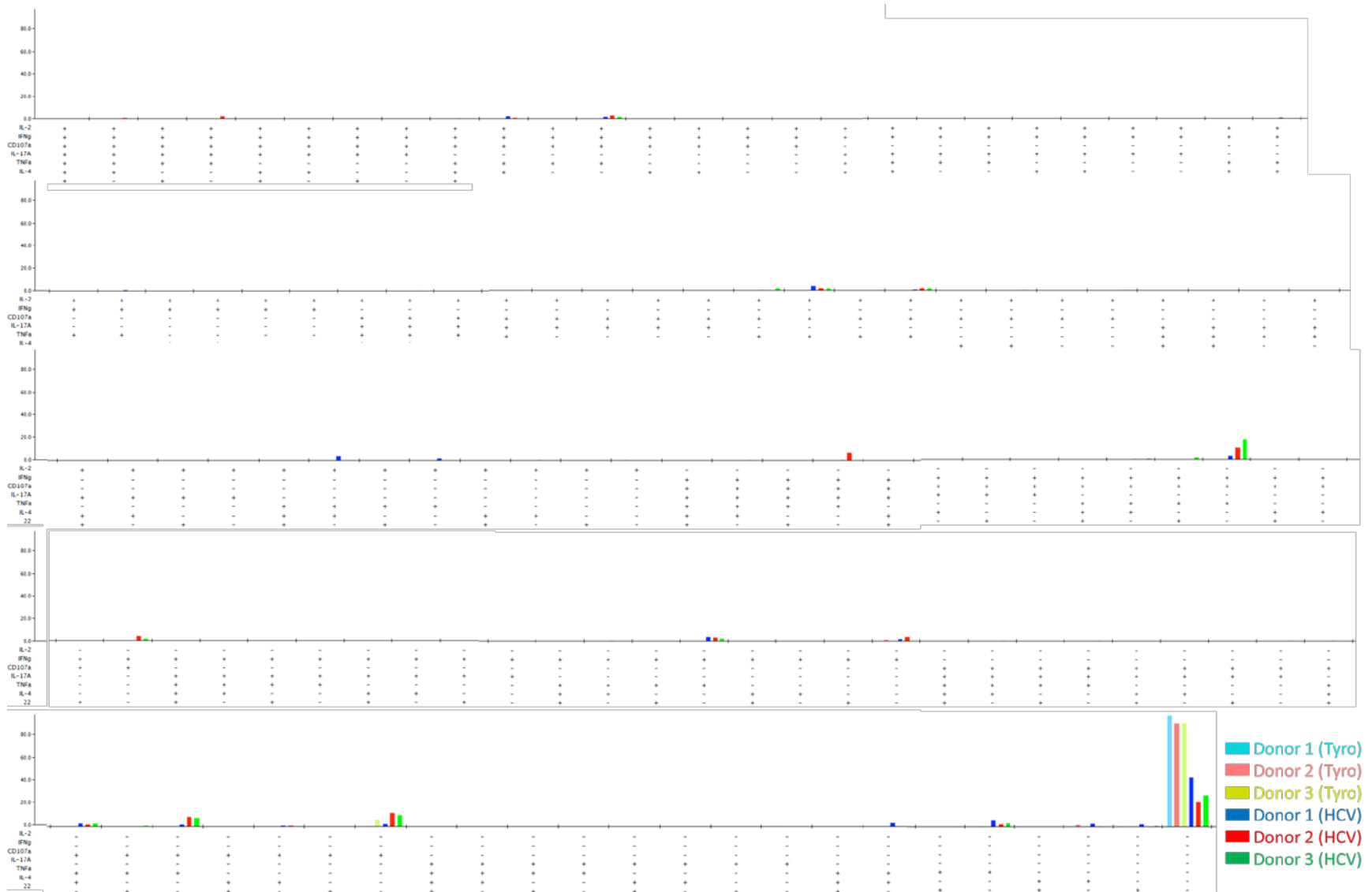
Timothy T. Spear, Yuan Wang, Thomas W. Smith Jr., Patricia E. Simms, Elizabeth Garrett-Mayer, Lance M. Hellman, Brian M. Baker, and Michael I. Nishimura

A

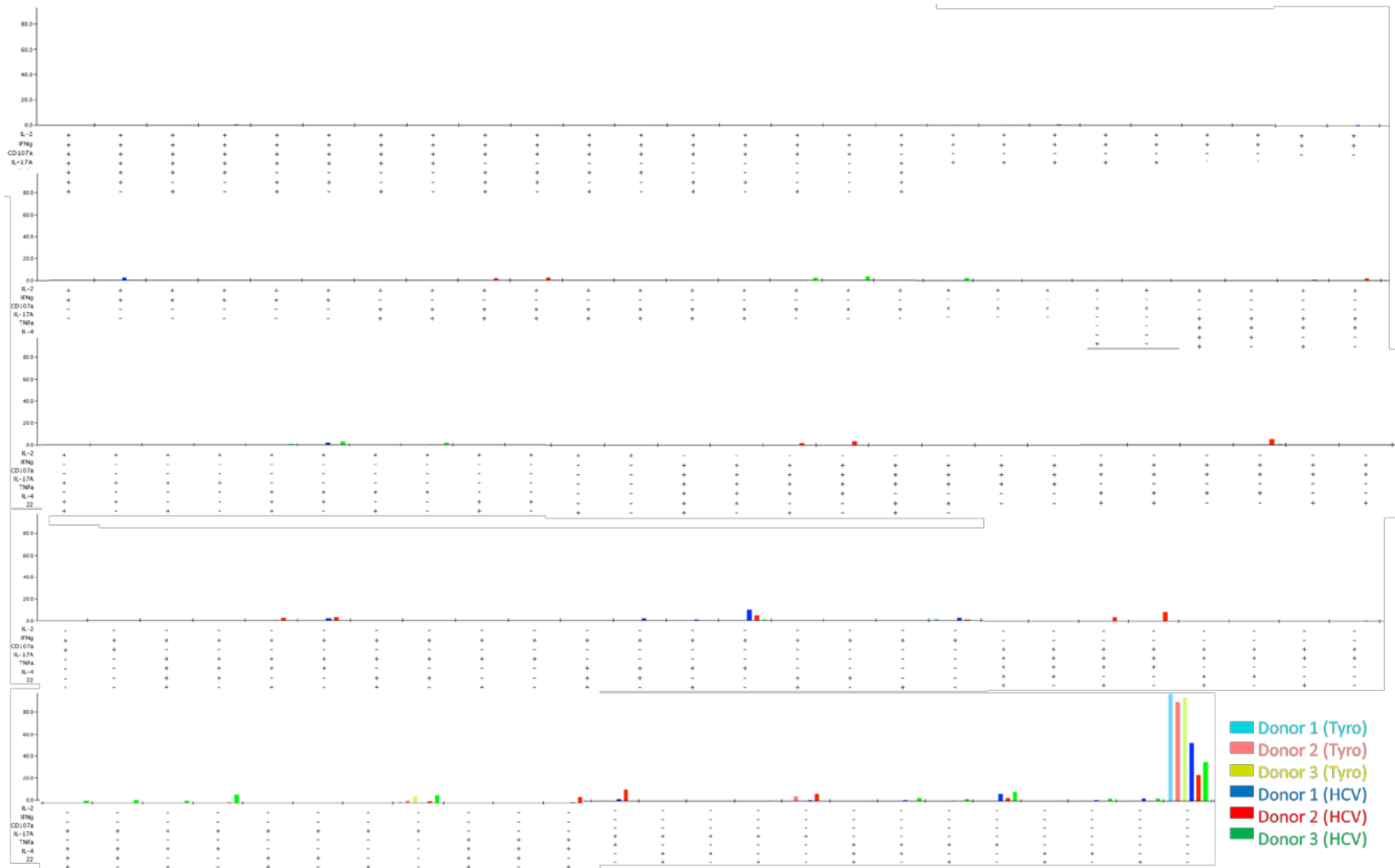
Supplementary Figure S1. SPICE-generated bar graphs comparing polyfunctional diversity of three PBL donor-derived T cells against WT HCV NS3:1406-1415 antigen. HCV1406 TCR-transduced T cells derived from PBL of three healthy donors were co-cultured for 5 hours with T2 cells loaded with 10 ug/mL of NS3:1406-1415 or tyrosinase:368-376 peptide. **(a)** CD8⁺ or **(b)** CD4⁺ T cells were evaluated CD107a, IFN γ , TNF α , IL-2, IL-4, IL-17A, and IL-22 expression by immunofluorescence. These complete graphs correspond to condensed versions in Figure 1c-d, which display phenotypes of >1% frequency in at least one donor. **(c)** and **(d)** represent respective plots generated without tyrosinase background subtraction displaying non-reactive populations.

B

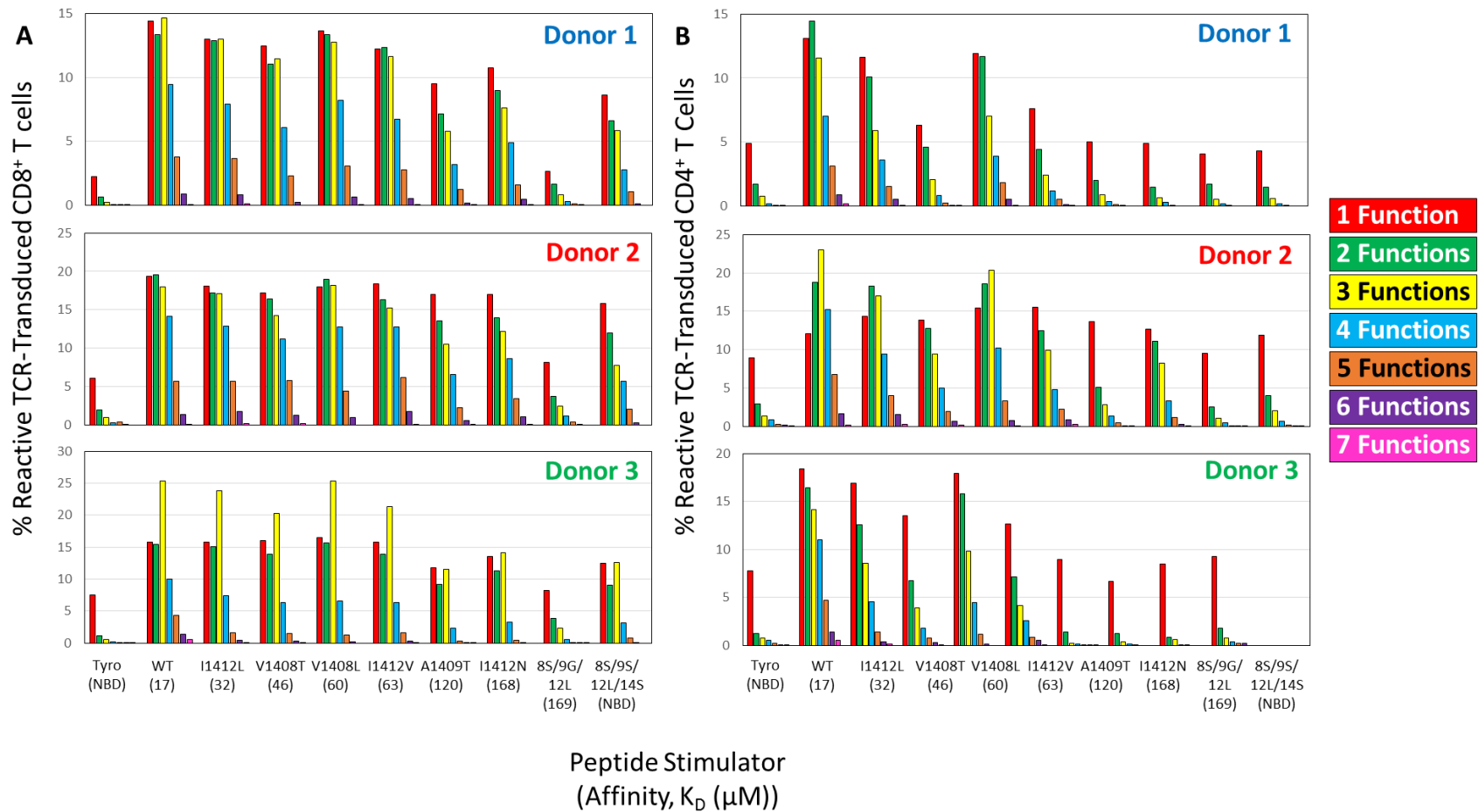
Supplementary Figure S1 (cont'd). SPICE-generated bar graphs comparing polyfunctional diversity of three PBL donor-derived T cells against WT HCV NS3:1406-1415 antigen. HCV1406 TCR-transduced T cells derived from PBL of three healthy donors were co-cultured for 5 hours with T2 cells loaded with 10 μ g/mL of NS3:1406-1415 or tyrosinase:368-376 peptide. **(a)** CD8⁺ or **(b)** CD4⁺ T cells were evaluated CD107a, IFN γ , TNF α , IL-2, IL-4, IL-17A, and IL-22 expression by immunofluorescence. These complete graphs correspond to condensed versions in Figure 1c-d, which display phenotypes of >1% frequency in at least one donor. **(c)** and **(d)** represent respective plots generated without tyrosinase background subtraction displaying non-reactive populations.

C

Supplementary Figure S1 (cont'd). SPICE-generated bar graphs comparing polyfunctional diversity of three PBL donor-derived T cells against WT HCV NS3:1406-1415 antigen. (c) frequency of polyfunctional CD8⁺ T cells stimulated with tyrosinase (negative control) or HCV WT peptide-loaded T2 cells, generated without negative control (tyrosinase) background subtraction.

D

Supplementary Figure S1 (cont'd). SPICE-generated bar graphs comparing polyfunctional diversity of three PBL donor-derived T cells against WT HCV NS3:1406-1415 antigen. (c) frequency of polyfunctional CD4⁺ T cells stimulated with tyrosinase (negative control) or HCV WT peptide-loaded T2 cells, generated without negative control (tyrosinase) background subtraction.



Supplementary Figure S2. Categorized polyfunctional phenotypes of HCV-stimulated TCR-transduced T cells. Includes negative control (tyrosinase) background reactivity for **(a)** CD8⁺ and **(b)** CD4⁺ T cells, corresponding to Figs. 2a-b.

in FlowJo. Resulting multivariate datasets were formatted and background subtracted (trypanase stimulation) in Pestle, and cool plot overlay was generated in SPICE. Evaluation along the x-axis (red box) determines frequency (shade of blue) of TCR-transduced cells for each of the 128 phenotypes. Each column is a separate phenotype denoted by +/- for each functional parameter. Evaluation along the y-axis (purple box) determines changes in frequency upon variant peptide stimulation for a given phenotype. Unique populations of simultaneously type 1 and type 2 cytokine producing cells are denoted in green boxes. Populations negative for IFN γ are surrounded by an orange box. TCR-pMHC interactions are ranked from bottom to top by decreasing affinity. Cool plots are representative of **(a)** Peptide-stimulated CD8⁺ T cells, Donor 1; **(b)** Peptide-stimulated CD4⁺ T cells, Donor 1; **(c)** Peptide-stimulated CD8⁺ T cells, Donor 2; **(d)** Peptide-stimulated CD8⁺ T cells (non-background subtracted), Donor 2; **(e)** Peptide-stimulated CD4⁺ T cells, Donor 2; **(f)** Peptide-stimulated CD4⁺ T cells, Donor 2 (non-background subtracted); **(g)** Peptide-stimulated CD8⁺ T cells, Donor 3; **(h)** Peptide-stimulated CD4⁺ T cells, Donor 3; **(i)** Tumor-stimulated CD8⁺ T cells, Donor 2; **(j)** Tumor-stimulated CD8⁺ T cells, Donor 2 (non-background subtracted); **(k)** Tumor-stimulated CD4⁺ T cells, Donor 2; **(l)** Tumor-stimulated CD4⁺ T cells, Donor 2 (non-background subtracted); **(m)** Tumor-stimulated CD8⁺ T cells, Donor 3; **(n)** Tumor-stimulated CD4⁺ T cells, Donor 3. Condensed plots in the text (Figure 3a-d) represent Supplementary Figure S1c,e,i,k, respectively.

F



Supplemental Figure S3 (cont'd). SPICE-generated cool plots comparing changing frequencies of T cell polyfunctional phenotypes against APL peptide and tumor stimulations. (f) Peptide-stimulated CD4⁺ T cells, Donor 2. Displays negative control (tyrosinase)-stimulated T cells without background subtraction. Full non-background subtracted plot shown in Figure 3b.

J



Supplemental Figure S3 (cont'd). SPICE-generated cool plots comparing changing frequencies of T cell polyfunctional phenotypes against APL peptide and tumor stimulations. (j) Tumor-stimulated CD8⁺ T cells, Donor 2. Displays negative control (HepG2)-stimulated T cells without background subtraction. Full non-background subtracted plot shown in Figure 3c.

K

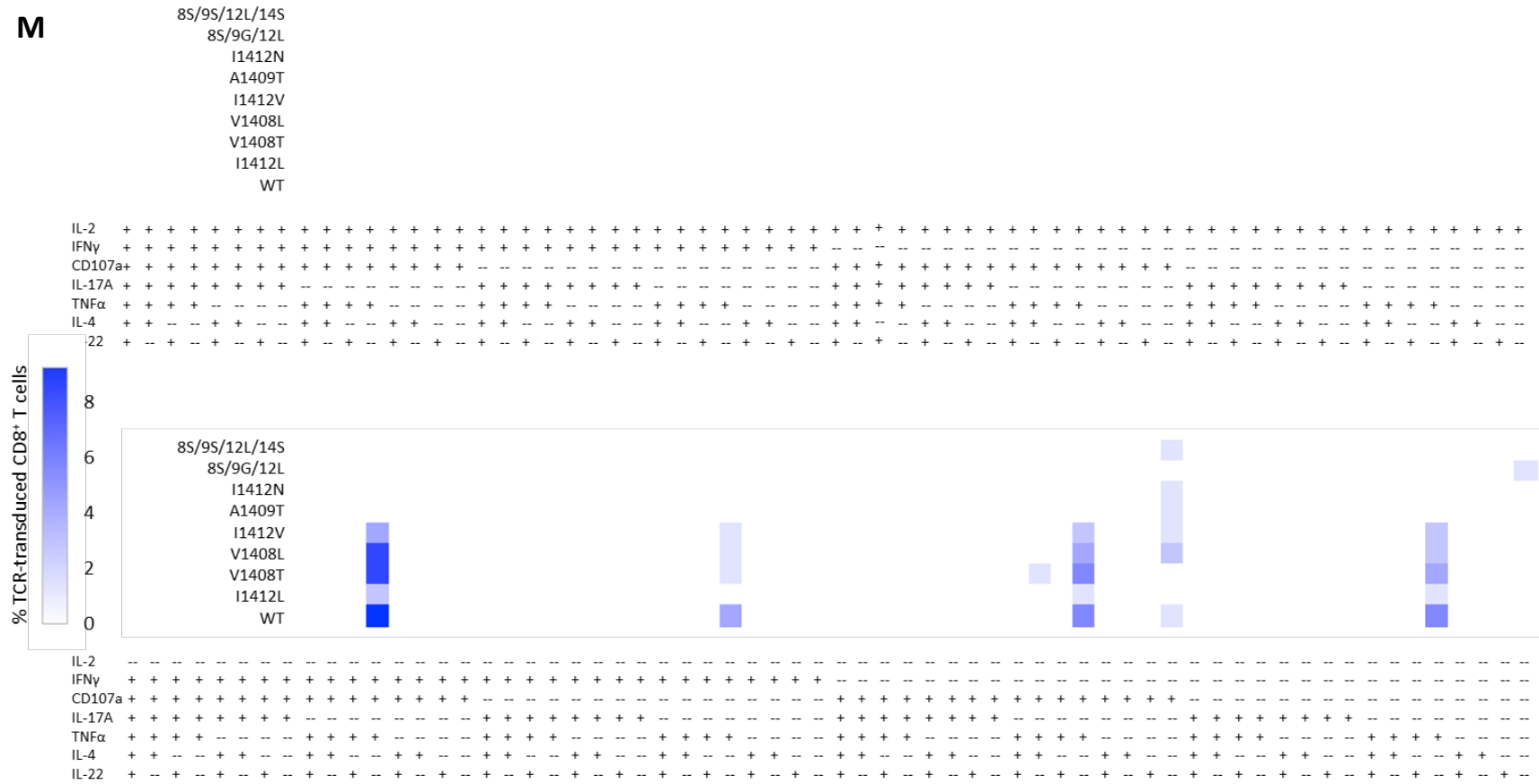


Supplemental Figure S3 (cont'd). SPICE-generated cool plots comparing changing frequencies of T cell polyfunctional phenotypes against APL peptide and tumor stimulations. (k) Tumor-stimulated CD4⁺ T cells, Donor 2. Full plot corresponds to Figure 3d.



Supplemental Figure S3 (cont'd). SPICE-generated cool plots comparing changing frequencies of T cell polyfunctional phenotypes against APL peptide and tumor stimulations. (I) Tumor-stimulated CD4⁺ T cells, Donor 2. Displays negative control (HepG2)-stimulated T cells without background subtraction. Full non-background subtracted plot shown in Figure 3d.

M

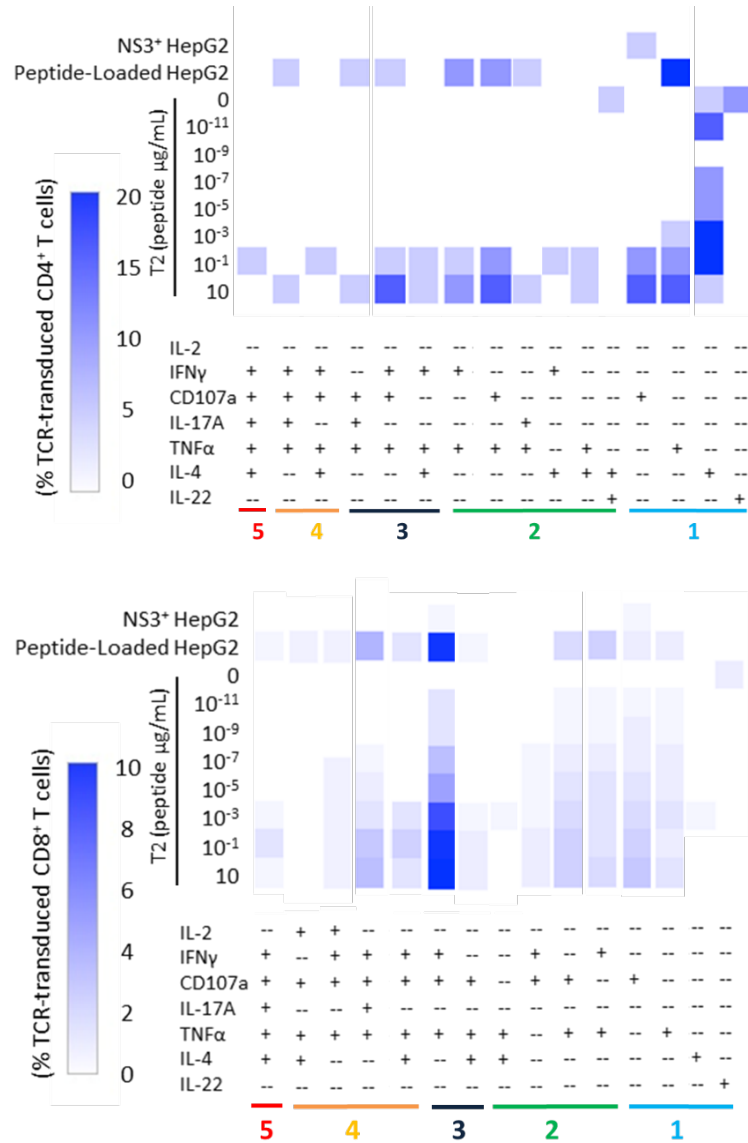


Supplemental Figure S3 (cont'd). SPICE-generated cool plots comparing changing frequencies of T cell polyfunctional phenotypes against APL peptide and tumor stimulations. (m) Tumor-stimulated CD8⁺ T cells, Donor 3

N

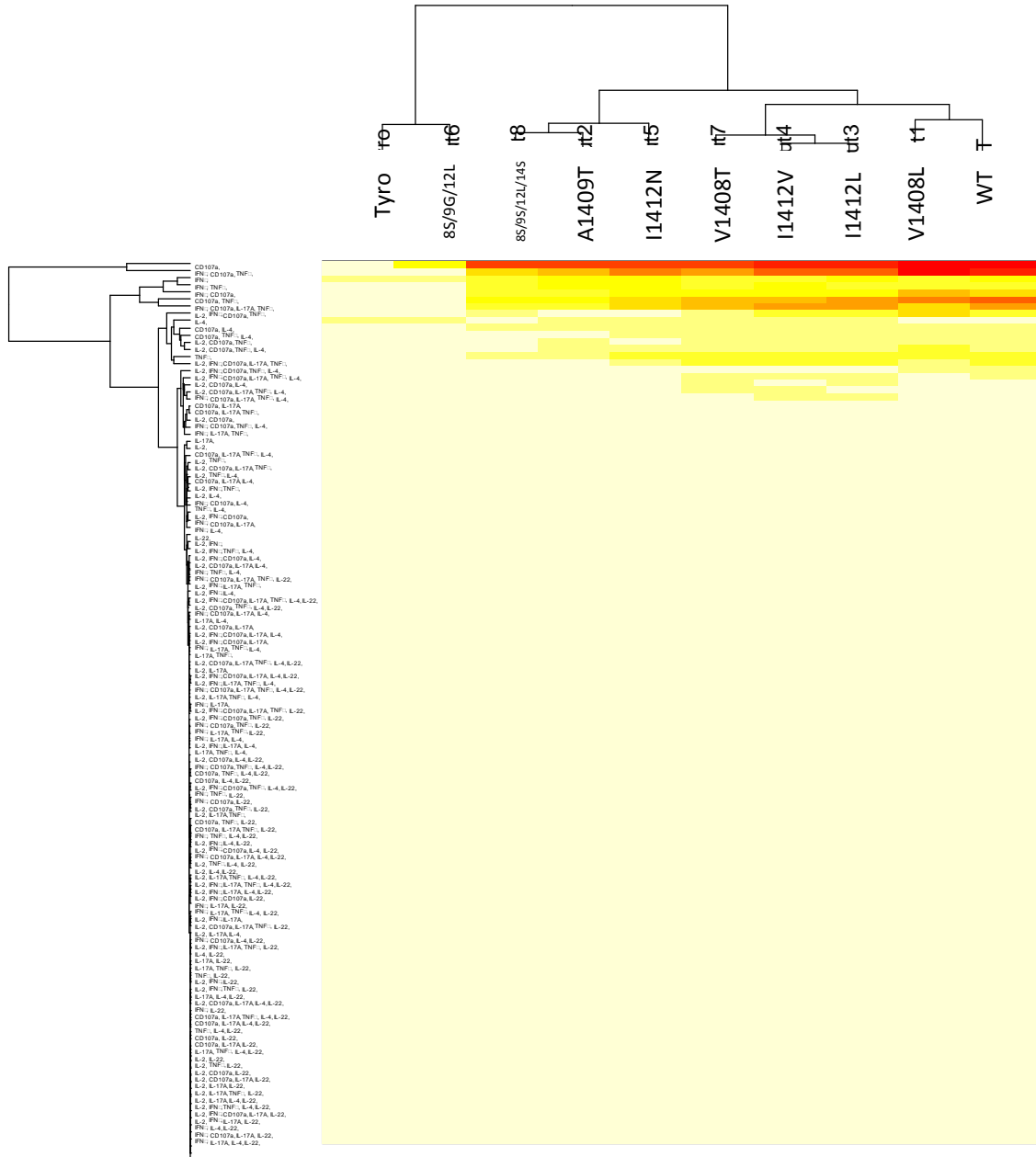


Supplemental Figure S3 (cont'd). SPICE-generated cool plots comparing changing frequencies of T cell polyfunctional phenotypes against APL peptide and tumor stimulations. (n) Tumor-stimulated CD4⁺ T cells, Donor 3



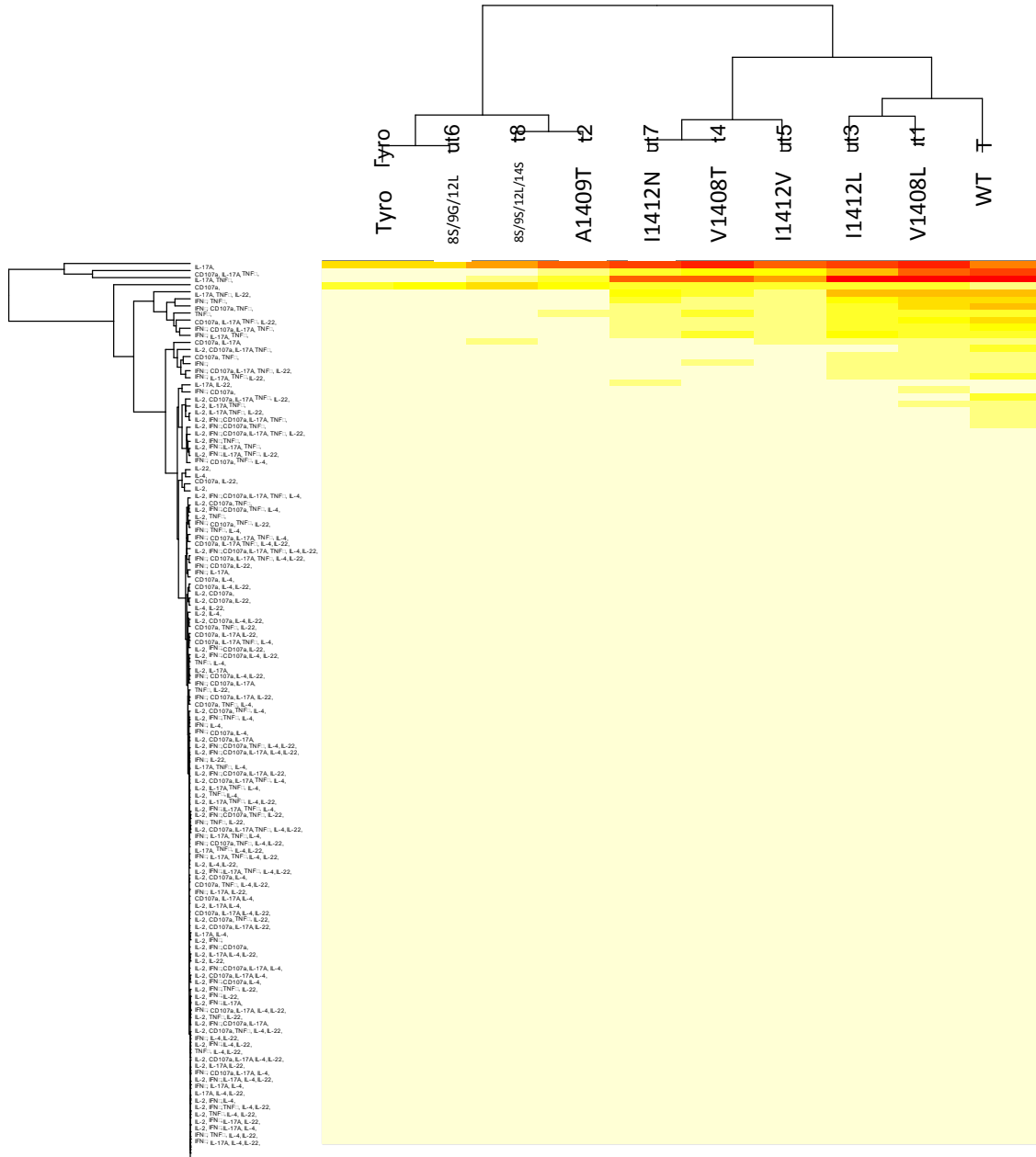
Supplementary Figure S4. Effects of peptide density on polyfunctional phenotypes. (a) CD4⁺ and (b) CD8⁺ HCV1406 TCR-transduced T cells were co-cultured with T2 cells loaded with WT HCV NS3:1406-1415 peptide ranging from 10 – 10⁻¹¹ µg/mL. T cells were also co-cultured with HepG2 cells expressing naturally processed full length NS3 protein or HepG2 cells exogenously loaded with 10 µg/mL NS3:1406-1415 peptide. Cells were evaluated for cytokine production and CD107a expression by immunofluorescence. As peptide concentration decreased, higher-order phenotypes (3+ functions) generally disappeared earlier. Additionally, loading HepG2 with peptide rescued maximal function, suggesting lower, less polyfunctional reactivity against tumor lines is a direct effect of lower antigen density.

A



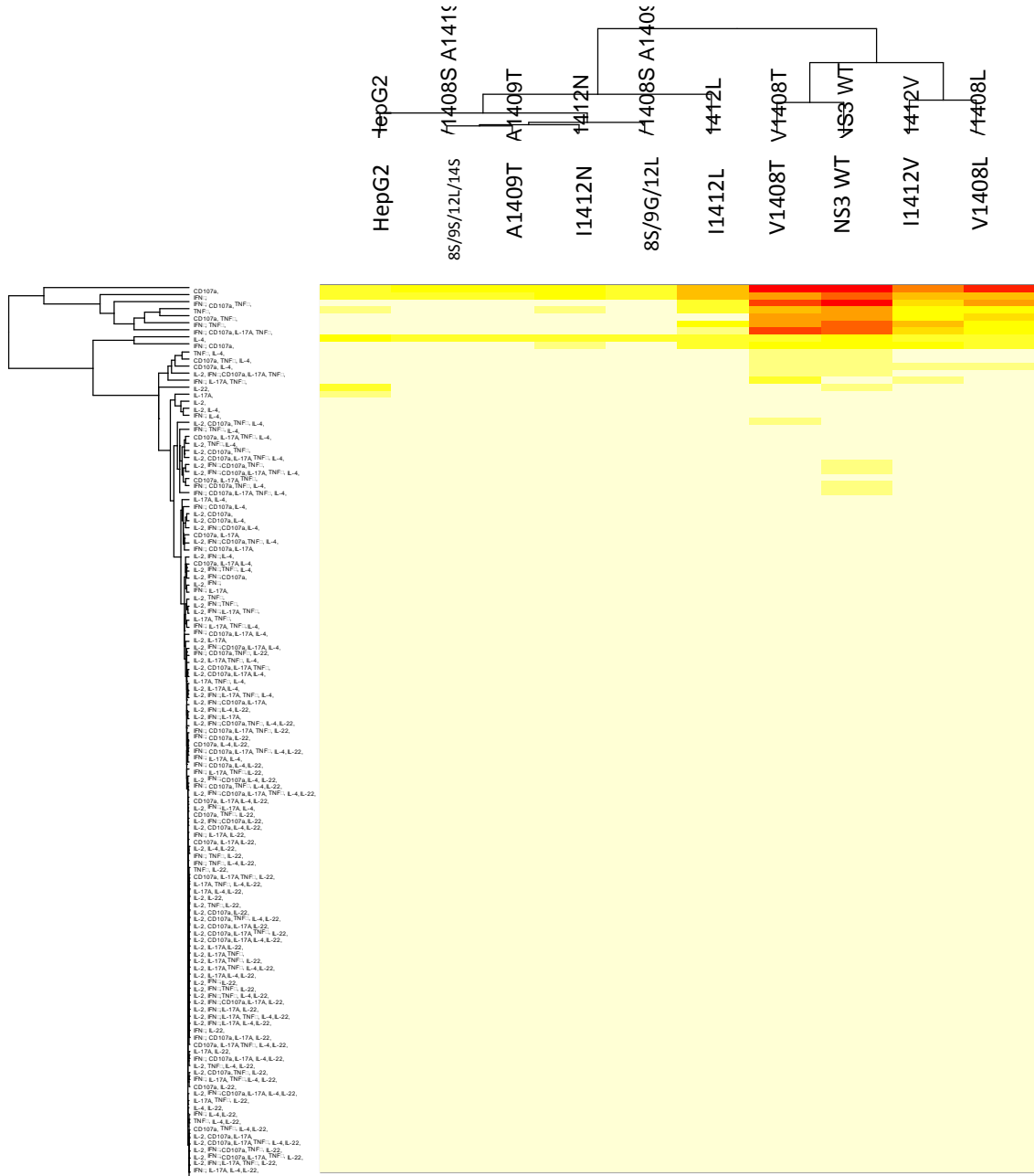
Supplementary Figure S5. Full hierarchical clustering maps. A hierarchical clustering analysis using FlowJo-generated Boolean gated frequencies demonstrates the functional relatedness between HCV NS3:1406-1415 APL stimulations. Full maps of **(a)** peptide-stimulated CD8⁺ T cells, **(b)** peptide-stimulated CD4⁺ T cells, and **(c)** tumor-stimulated CD8⁺ T cells to Figure 4a-c, respectively.

B



Supplementary Figure S5 (cont'd). Full hierarchical clustering maps. (b) peptide-stimulated CD4⁺ T cells. Full map corresponds to Figure 4b.

C



Supplementary Figure S5 (cont'd). Full hierarchical clustering maps. (c) tumor-stimulated CD8⁺ T cells. Full map corresponds to Figure 4c.